



Title	Influence of GaAs surface structure on tunneling anisotropic magnetoresistance and magnetocrystalline anisotropy in epitaxial Co <sub>50</sub> Fe <sub>50</sub> /n-GaAs junctions
Author(s)	Uemura, Tetsuya; Harada, Masanobu; Akiho, Takafumi; Matsuda, Ken-ichi; Yamamoto, Masafumi
Citation	Applied Physics Letters, 98(10), 102503 <a href="https://doi.org/10.1063/1.3561759">https://doi.org/10.1063/1.3561759</a>
Issue Date	2011-03-07
Doc URL	<a href="http://hdl.handle.net/2115/45102">http://hdl.handle.net/2115/45102</a>
Rights	Copyright 2011 American Institute of Physics. This article may be downloaded for personal use only. Any other use requires prior permission of the author and the American Institute of Physics. The following article appeared in Appl. Phys. Lett. 98, 102503 (2011) and may be found at <a href="https://dx.doi.org/10.1063/1.3561759">https://dx.doi.org/10.1063/1.3561759</a>
Type	article
File Information	APL98-10_102503.pdf



[Instructions for use](#)

# Influence of GaAs surface structure on tunneling anisotropic magnetoresistance and magnetocrystalline anisotropy in epitaxial $\text{Co}_{50}\text{Fe}_{50}/\text{n-GaAs}$ junctions

Tetsuya Uemura,<sup>a)</sup> Masanobu Harada, Takafumi Akiho, Ken-ichi Matsuda, and Masafumi Yamamoto

*Division of Electronics for Informatics, Hokkaido University, Sapporo 060-0814, Japan*

(Received 25 November 2010; accepted 13 February 2011; published online 8 March 2011)

An epitaxial  $\text{Co}_{50}\text{Fe}_{50}$  layer was grown on As-terminated or Ga-terminated GaAs, and the influence of the termination species on both uniaxial-type tunneling anisotropic magnetoresistance (TAMR) characteristics and magnetocrystalline anisotropy was investigated. The magnetocrystalline anisotropy induced in the  $\text{Co}_{50}\text{Fe}_{50}$  thin film was strongly dependent on the termination species of the GaAs surface, while the TAMR characteristics were almost unchanged. These experimental findings suggest that the TAMR effect is due to the anisotropy of electronic structure rather than the structural anisotropy. © 2011 American Institute of Physics. [doi:10.1063/1.3561759]

Spin-injection into semiconductors (SCs) has attracted much interest for future-generation spintronic devices, such as spin transistors<sup>1,2</sup> and spin light-emitting diodes.<sup>3</sup> In these devices, ferromagnet (F)/SC heterojunctions are used to create and detect a spin-polarized state in SCs. Thus, it is important to clarify the spin-dependent transport properties of F/SC junctions. We recently observed a tunneling anisotropic magnetoresistance (TAMR) effect in both  $\text{Co}_{50}\text{Fe}_{50}(\text{CoFe})/\text{n-GaAs}$  and  $\text{Co}_2\text{MnSi}/\text{n-GaAs}$  Schottky tunnel junctions.<sup>4,5</sup> The TAMR effect modulates the tunnel resistance depending on the absolute direction of the magnetization with respect to the crystal axes of the F. Since the TAMR occurs even for a single F/SC junction and produces a spin-valvelike magnetoresistance, it may affect the electrical detection of spin injection using F/SC heterojunctions. Thus, the origin of the TAMR effect and its influence on spin injection properties should be clarified.

The TAMR effect was first observed in a  $(\text{Ga},\text{Mn})\text{As}/\text{AlO}_x/\text{Au}$  tunnel junction,<sup>6</sup> and it has since been observed in several systems,<sup>4–12</sup> such as a  $\text{CoFe}/\text{MgO}/\text{CoFe}$  magnetic tunnel junction (MTJ),<sup>9</sup> a  $(\text{Co}/\text{Pt})/\text{AlO}_x/\text{Pt}$  tunnel junction,<sup>10</sup> and a  $\text{Fe}/\text{GaAs}/\text{Au}$  tunnel junction.<sup>11</sup> The origin of the TAMR, however, differs depending on the system. The TAMR effect produced in a  $(\text{Ga},\text{Mn})\text{As}$  tunnel junction has been attributed to the anisotropic density-of-states for tunneling electrons due to spin-orbit interactions (SOIs).<sup>6</sup> It was shown by first-principles calculations that the TAMR in an  $\text{Fe}/\text{MgO}/\text{Fe}$  MTJ is produced by a shift in the resonant surface states of an Fe energy band due to Rashba-SOI as the Fe magnetization rotates.<sup>13</sup> Moser *et al.*<sup>11</sup> observed uniaxial-type TAMR in a  $\text{Fe}/\text{GaAs}/\text{Au}$  tunnel junction, in which the tunnel resistance has 180°-symmetry for the angle of magnetization with respect to the GaAs [110] direction. Our results for  $\text{CoFe}/\text{n-GaAs}$  (Ref. 4) and  $\text{Co}_2\text{MnSi}/\text{n-GaAs}$  (Ref. 5) junctions are qualitatively similar to that for  $\text{Fe}/\text{GaAs}/\text{Au}$ .<sup>11</sup> Two possible origins for the uniaxial-type TAMR characteristics have been proposed:<sup>14</sup> (a) combination of Rashba-type and Dresselhaus-type SOIs and (b) uniaxial-type-strain-induced SOI. If the latter effect is the dominant origin of the

TAMR, the TAMR and magnetocrystalline anisotropy should be correlated since the strain induces magnetocrystalline anisotropy. The strain-induced SOI model was initially introduced to explain the TAMR in a  $(\text{Ga},\text{Mn})\text{As}/\text{AlO}_x/\text{Au}$  tunnel junction,<sup>6</sup> and correlation between the TAMR and magnetocrystalline anisotropy was experimentally demonstrated in a  $(\text{Ga},\text{Mn})\text{As}/\text{ZnSe}/(\text{Ga},\text{Mn})\text{As}$  MTJ.<sup>8</sup> Although we also observed both uniaxial-type TAMR and uniaxial-type magnetocrystalline anisotropy in  $\text{CoFe}/\text{n-GaAs}$  and  $\text{Co}_2\text{MnSi}/\text{n-GaAs}$  Schottky tunnel junctions,<sup>4,5,15,16</sup> the correlation between them was unclear. The purpose of this study is to clarify the correlation between the TAMR characteristics and magnetocrystalline anisotropy observed in a  $\text{CoFe}/\text{n-GaAs}$  Schottky junction. For that purpose we fabricated an epitaxial  $\text{CoFe}$  layer on As-terminated or Ga-terminated GaAs, and investigated the influence of the termination species on both TAMR characteristics and magnetocrystalline anisotropy.

Layer structures consisting of (from the substrate side) undoped GaAs (50 nm)/ $\text{n}^-$ -GaAs ( $\text{Si}=2 \times 10^{16} \text{ cm}^{-3}$ , 750 nm)/ $\text{n}^+$ -GaAs ( $\text{Si}=3 \times 10^{18} \text{ cm}^{-3}$ , 30 nm) were grown by molecular beam epitaxy at 580 °C on a GaAs(001) substrate. The  $\text{n}^+$ -GaAs layer was inserted to reduce the Schottky barrier width so that the tunnel conduction would be dominant. The sample was then capped with an arsenic protective layer and transported to an ultrahigh-vacuum magnetron-sputtering chamber with a base pressure of about  $6 \times 10^{-8}$  Pa. Prior to  $\text{CoFe}$  growth, the GaAs substrates were heated to obtain two kinds of surface reconstruction superstructures. As the substrate temperature increased, the arsenic coverage at the top of the (001) GaAs surface decreased, and surface reconstruction structures changed from  $c(4 \times 4)$  to As-stabilized  $(2 \times 4)$  and Ga-stabilized  $(4 \times 2)$  structures. The formation of As-stabilized  $(2 \times 4)$  or Ga-stabilized  $(4 \times 2)$  structure was confirmed by reflection high energy electron diffraction. Subsequently, a 20-nm-thick  $\text{CoFe}$  film was grown by magnetron sputtering at room temperature on either the As-stabilized surface (sample-A) or the Ga-stabilized surface (sample-B). The magnetocrystalline anisotropy of the  $\text{CoFe}$  thin film was investigated using a superconducting quantum interference device magnetometer

<sup>a)</sup>Electronic mail: uemura@ist.hokudai.ac.jp.

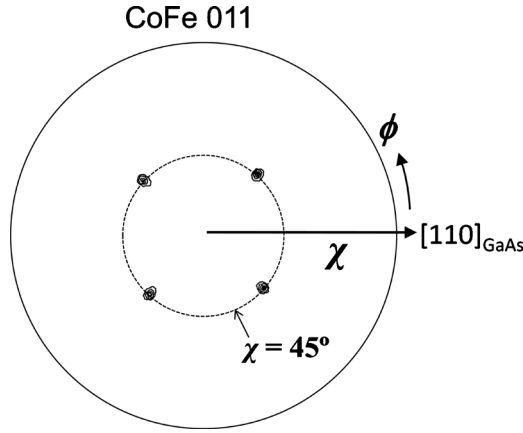


FIG. 1. X-ray pole figure of CoFe 011 diffraction for sample-A.

at 10 K. The TAMR characteristics of CoFe/n-GaAs Schottky junctions were measured at 4.2 K by the conventional four-probe method.

Figure 1 shows a pole figure of CoFe 011 diffraction for sample-A. The diffraction peaks showed fourfold symmetry with respect to the sample rotation angle,  $\phi$ , at a tilt angle,  $\chi$ , of  $45^\circ$ . Here, we set the GaAs[110] direction to the origin of  $\phi$ . We also obtained a similar result for sample-B (not shown). These results indicate that the CoFe thin film was epitaxially grown on the GaAs with a cube-on-cube relation for both sample-A and sample-B. Thus, the crystal axis direction described hereafter is common between CoFe and GaAs. Figure 2 shows the magnetic hysteresis curves of epitaxial CoFe films grown (a) on the As-stabilized GaAs surface (sample-A) and (b) on the Ga-stabilized GaAs surface (sample-B). A magnetic field was applied along the [110] and  $[1\bar{1}0]$  directions. A saturation magnetization of approximately  $1500 \text{ emu/cm}^3$  was obtained, a value comparable to that typically reported for the bulk sample. The CoFe films showed strong magnetic anisotropy for both samples. In addition to the cubic anisotropy imposed by the crystal symmetry of CoFe with easy axes of both [110] and  $[1\bar{1}0]$ , uniaxial anisotropy with an easy axis of either the [110] or  $[1\bar{1}0]$  direction was observed because of structural and/or electronic asymmetry of the CoFe/GaAs interface between [110] and  $[1\bar{1}0]$ , as discussed later. The magnetocrystalline energy of the CoFe thin film is given by

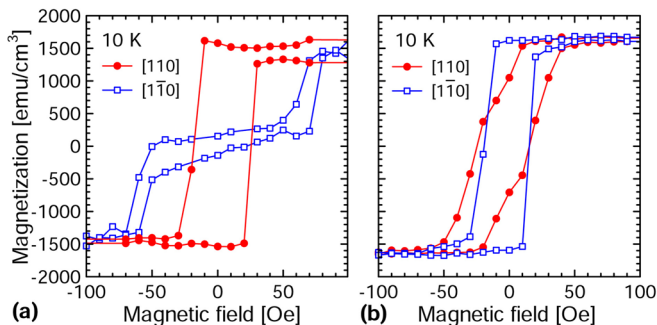


FIG. 2. (Color online) Magnetic hysteresis curves of epitaxial CoFe films grown (a) on the As-stabilized GaAs surface (sample-A) and (b) on the Ga-stabilized GaAs surface (sample-B). A magnetic field was applied along the [110] and  $[1\bar{1}0]$  directions.

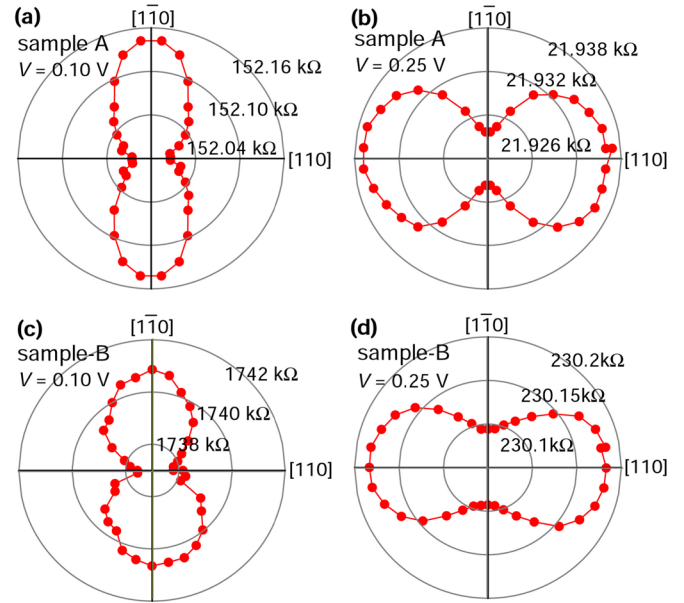


FIG. 3. (Color online) Polar plots of the tunnel resistance of a CoFe/n-GaAs Schottky junction with the As-stabilized n-GaAs surface (sample-A) biased at (a) 0.10 V and (b) 0.25 V, and with the Ga-stabilized n-GaAs surface (sample-B) biased at (c) 0.10 V and (d) 0.25 V. The bias voltage was defined with respect to the n-GaAs. The polar angle indicates the direction of magnetization with respect to the [110] direction.

$$E(\theta) = K_u \sin^2 \theta + K_1/4 \sin^2 2\theta, \quad (1)$$

where  $\theta$  is the angle of the magnetization ( $M$ ) direction of CoFe with respect to the [110] direction, and  $K_1$  and  $K_u$  are cubic and uniaxial anisotropy constants, respectively. The sign of  $K_u$  was positive (negative) for sample-A (B) because the easy axis direction for sample-A (B) was [110] ( $[1\bar{1}0]$ ). The fact that the sign of  $K_u$  changed between sample-A and sample-B indicates that the origin of the uniaxial anisotropy induced in the CoFe thin film was due to the difference of the surface reconstruction superstructures of GaAs. Such structural anisotropy could induce uniaxial-type strain with different directions between sample-A and sample-B.

Figure 3 shows polar plots of the tunnel resistance of a CoFe/n-GaAs Schottky junction with the As-stabilized n-GaAs surface (sample-A) biased at (a) 0.10 V and (b) 0.25 V, and with the Ga-stabilized n-GaAs surface (sample-B) biased at (c) 0.10 V and (d) 0.25 V. The bias voltage ( $V$ ) was defined with respect to the n-GaAs. The polar angle indicates the direction of an applied magnetic field of 1000 Oe, where the magnetization was forced to align along the magnetic field, with respect to the [110] direction. The tunnel resistance showed uniaxial-type anisotropy with respect to  $\theta$ , and is approximately given by

$$R(\theta) = (R_{1\bar{1}0} - R_{110}) \sin^2 \theta + R_{110} \equiv R_u \sin^2 \theta + R_{110}, \quad (2)$$

where  $R_{110}$  and  $R_{1\bar{1}0}$  are the tunnel resistance for  $M \parallel [110]$  and  $M \parallel [1\bar{1}0]$ , respectively, and  $R_u \equiv R_{1\bar{1}0} - R_{110}$ . The sign of  $R_u$  was positive at  $V=0.10 \text{ V}$  and negative at  $V=0.25 \text{ V}$  for both samples. Similar uniaxial-type anisotropy in the tunnel resistance has been observed in Fe/GaAs/Au junctions<sup>12</sup> and  $\text{Co}_2\text{MnSi/n-GaAs}$  junctions.<sup>5</sup> Figure 4 shows the bias-voltage dependence of  $R_u$  for CoFe/n-GaAs Schottky junctions with the As-stabilized n-GaAs surface (sample-A) and with the Ga-stabilized n-GaAs surface (sample-B).  $R_u$  was

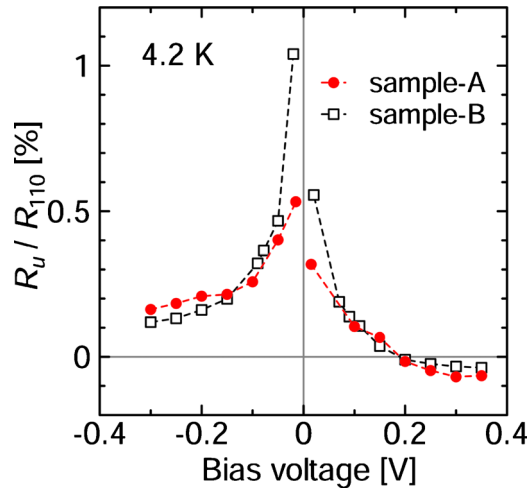


FIG. 4. (Color online) Bias-voltage dependence of the normalized  $R_u$ , defined by  $(R_{1\bar{1}0} - R_{110})/R_{110}$ , of CoFe/n-GaAs Schottky junctions with the As-stabilized n-GaAs surface and with the Ga-stabilized n-GaAs surface (sample-B), where  $R_{110}$  and  $R_{1\bar{1}0}$  stand for the tunnel resistance when the magnetization of the CoFe electrode orients to the  $[110]$  and  $[1\bar{1}0]$  directions, respectively.

obtained by measuring  $R_{110}$  and  $R_{1\bar{1}0}$  at each bias voltage, and it was normalized by  $R_{110}$ . The figure clearly shows that the sign of  $R_u$  is strongly dependent on the bias-voltage, and that it changed at  $V \approx 0.16$  V; however, it was insensitive to any difference in the GaAs surface's superstructure. This contrasted with the magnetocrystalline anisotropy result.

We will discuss the origin of the uniaxial-type TAMR effect. Matos-Abiague *et al.*<sup>14</sup> proposed a theoretical model to explain the uniaxial-type TAMR characteristics: (a) combination of both Rashba-type and Dresselhaus-type SOIs and (b) uniaxial-type-strain-induced SOI. In both cases, the Hamiltonian of SOIs for tunneling electrons has the same form, given by

$$H_{\text{SOI}} = \alpha(\sigma_x k_y - \sigma_y k_x) + \beta(\sigma_x k_x - \sigma_y k_y), \quad (3)$$

for Rashba and Dresselhaus-type SOIs, and by

$$H_{\text{SOI}} = \eta(\sigma_x k_y - \sigma_y k_x) + \mu(\sigma_x k_x - \sigma_y k_y), \quad (4)$$

for uniaxial-type-strain-induced SOIs. Here,  $\alpha$  and  $\beta$  are the effective Rashba and Dresselhaus parameters,  $\eta$  and  $\mu$  are effective strain tensor components under uniaxial-type strain with respect to the  $[110]$  or  $[1\bar{1}0]$  direction,  $\sigma_x$ ,  $\sigma_y$ ,  $\sigma_z$  are the Pauli spin matrices, and  $k_x$ ,  $k_y$  are the electron wave vector components. The  $x$ -axis and  $y$ -axis are set to the  $[100]$  and  $[010]$  direction, respectively, and the  $z$ -axis is set to the tunneling direction. These SOIs produce anisotropic SOI fields, resulting in a uniaxial-type TAMR, and  $R_u$  is proportional to  $\alpha \cdot \beta$  or  $\eta \cdot \mu$ .

The result shown in Fig. 2 that the sign of  $K_u$  changed depending on the surface reconstruction superstructures of GaAs indicates that the sign of  $\eta \cdot \mu$  changed between sample-A and sample-B. The sign of  $R_u$ , however, was in-

sensitive to the surface reconstruction superstructures, as shown in Fig. 4. This result indicates that  $R_u$  is dominantly proportional to  $\alpha \cdot \beta$  instead of  $\eta \cdot \mu$ . This model also explains the bias-voltage dependence of  $R_u$ . The strain tensor components, in general, are almost constant against the bias-voltage. Thus, if  $R_u$  is proportional to  $\eta \cdot \mu$ , the strong bias-voltage dependence of  $R_u$  shown in Fig. 4 cannot be explained. On the other hand, the sign and magnitude of  $\alpha$  would be voltage-dependent, since  $\alpha$  is proportional to the strength of the  $z$ -component of the electric field at the F/n-GaAs interface. Thus, one can qualitatively explain the bias-voltage dependence of  $R_u$ , if  $R_u$  is assumed to be proportional to  $\alpha \cdot \beta$ .

In summary, we found there is no direct correlation between magnetocrystalline anisotropy and TAMR in a CoFe/n-GaAs Schottky junction, and that the uniaxial-type magnetocrystalline anisotropy induced in a CoFe thin film grown on GaAs is attributable to the uniaxial-type strain between CoFe and GaAs, while the uniaxial-type TAMR mainly originates from the combination of Rashba-type and Dresselhaus-type SOIs.

This work was partly supported by Grants-in-Aid for Scientific Research (Grant Nos. 20246054, 21360140, and 22560001) and a Grant-in-Aid for Scientific Research on Priority Area "Creation and control of spin current" (Grant No. 19048001), from the MEXT, Japan.

<sup>1</sup>S. Datta and B. Das, *Appl. Phys. Lett.* **56**, 665 (1990).

<sup>2</sup>S. Sugahara and M. Tanaka, *Appl. Phys. Lett.* **84**, 2307 (2004).

<sup>3</sup>A. T. Hanbicki, O. M. J. van't Erve, R. Magno, G. Kioseoglou, C. H. Li, B. T. Jonker, G. Itskos, R. Mallory, M. Yasar, and A. Petrou, *Appl. Phys. Lett.* **82**, 4092 (2003).

<sup>4</sup>T. Uemura, Y. Imai, M. Harada, K.-i. Matsuda, and M. Yamamoto, *Appl. Phys. Lett.* **94**, 182502 (2009).

<sup>5</sup>T. Uemura, M. Harada, K.-i. Matsuda, and M. Yamamoto, *Appl. Phys. Lett.* **96**, 252106 (2010).

<sup>6</sup>C. Gould, C. Rüster, T. Jungwirth, E. Girgis, G. M. Schott, R. Giraud, K. Brunner, G. Schmidt, and L. W. Molenkamp, *Phys. Rev. Lett.* **93**, 117203 (2004).

<sup>7</sup>C. Rüster, C. Gould, T. Jungwirth, J. Sinova, G. M. Schott, R. Giraud, K. Brunner, G. Schmidt, and L. W. Molenkamp, *Phys. Rev. Lett.* **94**, 027203 (2005).

<sup>8</sup>H. Saito, S. Yuasa, and K. Ando, *Phys. Rev. Lett.* **95**, 086604 (2005).

<sup>9</sup>L. Gao, X. Jiang, S. Yang, J. D. Burton, E. Y. Tsymlal, and S. S. P. Parkin, *Phys. Rev. Lett.* **99**, 226602 (2007).

<sup>10</sup>B. G. Park, J. Wunderlich, D. A. Williams, S. J. Joo, K. Y. Jung, K. H. Shin, K. Olejnik, A. B. Shick, and T. Jungwirth, *Phys. Rev. Lett.* **100**, 087204 (2008).

<sup>11</sup>J. Moser, A. Matos-Abiague, D. Schuh, W. Wegscheider, J. Fabian, and D. Weiss, *Phys. Rev. Lett.* **99**, 056601 (2007).

<sup>12</sup>T. Inokuchi, T. Marukame, M. Ishikawa, H. Sugiyama, and Y. Saito, *Appl. Phys. Express* **2**, 023006 (2009).

<sup>13</sup>A. N. Chantis, K. D. Belashchenko, E. Y. Tsymlal, and M. van Schilf-gaarde, *Phys. Rev. Lett.* **98**, 046601 (2007).

<sup>14</sup>A. Matos-Abiague, M. Gmitra, and J. Fabian, *Phys. Rev. B* **80**, 045312 (2009).

<sup>15</sup>T. Uemura, Y. Imai, S. Kawagishi, K.-i. Matsuda, and M. Yamamoto, *Physica E (Amsterdam)* **40**, 2025 (2008).

<sup>16</sup>S. Kawagishi, T. Uemura, Y. Imai, K.-i. Matsuda, and M. Yamamoto, *J. Appl. Phys.* **103**, 07A703 (2008).